APPLIED AND ENVIRONMENTAL MICROBIOLOGY, Mar. 2003, p. 1702–1709 Vol. 69, No. 3
0099-2240/03/$08.00+0 DOI: 10.1128/AEM.69.3.1702–1709.2003

Mass Transport of Macromolecules within an In Vitro Model of Supragingival Plaque

Thomas Thurnheer,* Rudolf Gmür, Stuart Shapiro,† and Bernhard Guggenheim

Institute for Oral Microbiology and General Immunology, University of Zürich, CH-8028 Zürich, Switzerland

Received 26 June 2002/Accepted 3 December 2002

The aim of this study was to examine the diffusion of macromolecules through an in vitro biofilm model of supragingival plaque. Polyspecies biofilms containing *Actinomyces naeslundii*, *Fusobacterium nucleatum*, *Streptococcus oralis*, *Streptococcus sobrinus*, *Veillonella dispar*, and *Candida albicans* were formed on sintered hydroxyapatite disks and then incubated at room temperature for defined periods with fluorescent markers with molecular weights ranging from 3,000 to 900,000. Subsequent examination by confocal laser scanning microscopy revealed that the mean square penetration depths for all tested macromolecules except immunoglobulin M increased linearly with time, diffusion coefficients being linearly proportional to the cube roots of the molecular weights of the probes (range, 10,000 to 240,000). Compared to diffusion in bulk water, diffusion in the biofilms was markedly slower. The rate of diffusion for each probe appeared to be constant and not a function of biofilm depth. Analysis of diffusion phenomena through the biofilms suggested tortuosity as the most probable explanation for retarded diffusion. Selective binding of probes to receptors present in the biofilms could not explain the observed extent of retardation of diffusion. These results are relevant to oral health, as selective attenuated diffusion of fermentable carbohydrates and acids produced within dental plaque is thought to be essential for the development of carious lesions.

The structure of microbial biofilms, consisting of single cells, cell aggregates, and microcolonies embedded in an exocellular polymeric hydrogel, has been the subject of intense experimental and theoretical scrutiny over the past decade (10, 20, 38, 46). Biofilm anatomy and the physiological status of the cells contained within biofilms have profound consequences for clinical, industrial, and environmental microbiology. The exocellular space constitutes a primitive microcirculatory system that enables two-way transport between biofilm constituents and their surroundings and that facilitates intrabiofilm communication.

Knowledge of the kinetics of mass transport within biofilms is essential for understanding how they achieve their characteristic architectures and for optimizing strategies to control or eradicate biofilms. Transport phenomena in biofilms have been studied by using microelectrodes (3, 41, 42) fiberoptic microsensors (2, 43), nuclear magnetic resonance spectroscopy (1, 52), infrared spectroscopy combined with Raman microscopy (47), fluorescence recovery after photobleaching (4, 5), fluorescence correlation spectroscopy (FCS) (18), and confocal laser scanning microscopy (CLSM) (11, 25, 26). Indirect methods predicated upon nuclear magnetic resonance spectroscopy, infrared spectroscopy-Raman microscopy, fluorescence recovery after photobleaching, FCS, or CLSM are preferred for measuring mass transport in biofilms, since invasive procedures (e.g., those involving microelectrodes or microsensors) are likely to compromise structural integrity and therefore perturb the delicate systems that investigators seek to monitor.

Dental plaques are naturally occurring biofilms involved in the development of caries and periodontal diseases. The diffusion of carbohydrates into supragingival plaque and of metabolites within biofilms into the exterior milieu is crucial for carious lesion formation (8, 12, 30, 32, 48). In this study, we sought to quantify mass transport within a recently described polyspecies biofilm model of supragingival plaque (16).

MATERIALS AND METHODS

Preparation of biofilms. *Actinomyces naeslundii* OMZ 745, *Veillonella dispar* ATCC 17748^T (OMZ 493), *Fusobacterium nucleatum* KP-F2 (OMZ 596), *Streptococcus sobrinus* OMZ 176, *Streptococcus oralis* SK248 (OMZ 607), and *Candida albicans* OMZ 110 were used as inocula for biofilm formation (16, 45). Biofilms were grown on sintered hydroxyapatite (HA) disks (diameter, 10.6 mm) in 24-well polystyrene cell culture plates as described previously (16), except that the ratio of saliva to modified fluid universal medium (mFUM) was 70:30 (vol/vol) instead of 50:50 (vol/vol) (45); mFUM is fluid universal medium (15) modified by the addition of 67 mmol of Sørensen buffer/liter [final pH, 7.2]). Pellicle-coated disks (16, 45) were covered with 1.6 ml of 70% saliva–30% mFUM. The carbohydrate concentration in mFUM was 0.3% (wt/vol), and the carbohydrate was either glucose (biofilm cultivation from 0 to 16.5 h) or a 1:1 (wt/wt) mixture of glucose and sucrose (biofilm cultivation from 16.5 h to 64.5 h). Wells were inoculated with mixed cell suspensions (200 μl) prepared from equal volumes of the various species (optical density at 550 nm of each species, 1.0 ± 0.05 [range of acceptible values]) and incubated anaerobically at 37°C. The medium was replenished after dipping (see below) at 16.5 and 40.5 h by aspirating spent medium and adding fresh medium (1.6 ml of 70:30 [vol/vol] saliva-mFUM). At 16.5, 20.5, 24.5, 40.5, 44.5, 48.5, and 64.5 h, biofilms were washed by three consecutive dips in 2 ml of sterile physiological saline (1 min per dip, room temperature [20 to 23°C]). After the 64.5-h dip, biofilms were stored in physiological saline until further use.

Staining of bacteria and EPS in biofilms. Cells in biofilms were stained by incubation at room temperature for 30 min with a 0.3% solution of Syto13 (Molecular Probes B. V., Leiden, The Netherlands) in physiological saline. Exocellular polymeric substances (EPS) were stained by incubating biofilms for 3 h with Calcofluor (Sigma Chemical Co., Buchs, Switzerland; 10 μg ml^{-1} in 10 mM sodium phosphate [pH 7.5]).

* Corresponding author. Mailing address: Institute for Oral Microbiology and General Immunology, University of Zürich, Plattenstr. 11, CH-8028 Zürich, Switzerland. Phone: 41 1 634 3256. Fax: 41 1 634 4310. E-mail: thurnher@zzmk.unizh.ch.

† Present address: Basilea Pharmaceutica AG, CH-4002 Basel, Switzerland.

Incubation of biofilms with fluorescent mass transport probes. Rinsed HA disks covered with 64.5-h biofilms were immersed in solutions of the following fluorescent probes at room temperature: neutral Texas red (TR)-conjugated dextrans (TR-dextrans; Molecular Probes; 0.2 mg/ml) with mean molecular weights of 3,000 (3K-Dex; product no. D-3329), 10,000 (10K-Dex; product no. D-1828), 40,000 (40K-Dex; product no. D-1829), and 70,000 (70K-Dex; product no. D-1819); TR-conjugated whole immunoglobulin G (IgG) with a molecular weight of ~150,000 (150K-Ig; Milan Analytica S.A., La Roche, Switzerland; product no. 115-075-003; 0.03 mg/ml); TR-conjugated $F(ab')_2$ fragments of IgG with a molecular weight of ~100,000 (100K-Ig; Milan Analytica; product no. 115-076-003; 0.03 mg/ml); and R-phycoerythrin with a molecular weight ~240,000 (240K-PE; Molecular Probes; product no. P-801; 4 mg/ml). Immediately after incubation with the fluorescent probes for 2, 60, 120, 300, or 600 s, disks were washed by two 60-s dips in physiological saline at room temperature. All experiments were repeated three times with biofilms produced on separate occasions.

Additional experiments were performed with IgM monoclonal antibody 396AN1 (molecular weight, ~900,000; 900K-Ig) (50) conjugated to Alexa Fluor594 (Molecular Probes; product no. A20185), Nile red-coated polystyrene microspheres (diameter, 0.02 μm; Molecular Probes; product no. F-8784; 0.2 mg/ml), and anionic fluorescein-conjugated dextrans with molecular weights of 4,000 and 70,000 (Fluka Chemie AG, Buchs, Switzerland; product no. 46944 and 46945, respectively; 0.2 mg/ml). 900K-Ig and Nile red-coated microspheres were incubated with biofilms for 90 min.

To test for the binding of dextrans to biofilms, biofilms were preincubated with unlabeled dextran (molecular weight, 1,000; Fluka Chemie; product no. 31416) for 10 min and washed by two 60-s dips in physiological saline. Biofilms then were reincubated with TR-dextrans and processed as described above.

After dip washing, excess saline was aspirated gently from the disks without touching the biofilms, and the disks were embedded upside down in 20 μl of Mowiol (17). Embedded disks were stored at room temperature in the dark for at least 6 h prior to microscopic examination. Dip washing failed to displace dyes that had already penetrated the biofilm, and embedding in Mowiol blocked further diffusion of probes through the biofilm.

Microscopy and image analysis. Stained biofilms were examined using a DM IRB E inverted microscope (Leica Mikroskopie GmbH, Wetzlar, Germany) fitted with a UV laser (Coherent Inc., Santa Clara, Calif.), an He-Ne laser (Uniphase Vertriebs GmbH, Eching/Munich, Germany), an Ar laser (Coherent Inc.), and a TCS SP2 computer-operated confocal laser scanning system (Leica Lasertechnik GmbH, Heidelberg, Germany). Filters were set to 400 to 490 nm for detection of Calcofluor, 520 to 540 nm for fluorescein and Syto13, and 595 to 660 nm for TR, Alexa Fluor594, Nile red, and R-phycoerythrin. Confocal images were obtained by using ×40 (numeric aperture, 1.25; zoom factor, 2.5) and ×100 (numeric aperture, 1.4) oil immersion objectives. Each biofilm was scanned at five randomly selected positions not close to the disk edge. *z* series were generated by vertical optical sectioning at each of these positions; the thickness of each section was 1.018 μm. Image acquisition was done in the ×6 line average mode, and the data were processed on a Silicon Graphics (Mountain View, Calif.) 320 visual workstation fitted with Windows NT version 4.0. Scans were recombined by using Imaris 3.1 software (Bitplane AG, Zürich, Switzerland). The depths of probe penetration into biofilms were calculated by multiplying the number of stained *z* sections by 1.018 μm.

Viscometry. The viscosity of the 70:30 saliva-mFUM biofilm cultivation medium was measured at room temperature by using an Ubbelohde capillary viscometer (Schott capillary no. 0a; Digitana AG, Horgen, Switzerland) according to the instructions of the manufacturer.

Diffusion coefficients. The calculation of diffusion coefficients is based on the following theoretical background. Diffusion results from the stochastic movement of molecules due to thermal vibrations. The mean square displacement ($\bar{x}^2$) for rigid spheres over a brief time interval (Δt) due to Brownian motion was shown independently by Einstein (14) and von Smoluchowski (51) to be

$$\bar{x}^2 = \frac{kT\Delta t}{3\pi\eta r} \tag{1}$$

where k is Boltzmann's constant, r is the hydrodynamic radius of the molecule, T is the absolute temperature, and η is the shear viscosity of the medium.

According to Fick's first law of diffusion, the flux (J) of molecules passing through a defined surface during a given time is proportional to the concentration gradient ($\partial C/\partial z$) normal to that surface, as follows:

$$J_z = -D\left(\frac{\partial C}{\partial z}\right) \tag{2}$$

where D is the diffusion coefficient for the molecule of interest, C is the concentration of the diffusing substance, and z is the distance from the diffusion surface. Einstein (14) showed that $\bar{x}^2$ is related to D by the equation

$$\bar{x}^2 = 2D\Delta t \tag{3}$$

Combining equations 1 and 3 yields the Stokes-Einstein equation

$$D = \frac{kT}{6\pi\eta r} \tag{4}$$

It is assumed, as a first approximation, that the biofilm covering a disk is cylindrical. The surface available for entry of the dye consists of the vertical border and the top of the cylinder. Since HA disks have a diameter of 10.6 mm and 64.5-h biofilms have a maximum height of 50 μm, it can be calculated that >98% of the dye must enter the biofilm through the top surface. Therefore, net mass transport of dye into the biofilm can be regarded as a unidimensional phenomenon parallel to the surface of the biofilm. Experimental biofilm diffusion coefficients (D_{bf}) for each probe were determined by using weighted least-squares regression (49) of $\bar{x}^2$ versus Δt.

RESULTS

Figure 1 provides an impression of the composition of the artificial supragingival plaque biofilm at 64.5 h and the distributions of cells, EPS, and interstitial voids. The biofilm thickness at 64.5 h was 30 ± 10 μm (mean and standard deviation).

Images of the penetration of 10K-Dex into artificial supragingival plaque as a function of time are shown in Fig. 2. After 2 s, the probe was confined largely to the superficial layer of the biofilm, with progressive migration of the probe to greater depths with longer incubation periods. After 120 s, the probe appeared to have extended approximately half way through the biofilm, and by 600 s, 10K-Dex was distributed throughout much of the volume of the biofilm in an anisotropic manner consistent with the structural heterogeneity revealed in Fig. 1. Probe penetration into substratal regions occurred to a lesser extent than did that into superficial regions, and throughout the biofilm, "lakes" and "holes" corresponding to areas of high and low levels of probe penetration, respectively, were readily apparent.

The diffusion into biofilms of probes ranging in molecular weight from 3,000 (3K-Dex) to 240,000 (240K-PE) is depicted in Fig. 3 (incubation time for 3K-Dex, 120 s; incubation time for the other probes, 600 s). Whereas 3K-Dex was distributed throughout the whole biofilm by 120 s and 10K-Dex was so distributed by 600 s, both 40K-Dex and 70K-Dex were largely confined to the upper half of the biofilm by 600 s. Only slight penetration was observed for the 100K-Ig, 150K-Ig, and 240K-PE probes by 600 s, although small lakes of 240K-PE were seen by 600 s in substratal regions. However, even after 90 min, neither Alexa Fluor594-conjugated 900K-Ig nor Nile red-coated microspheres (0.02 μm) succeeded in penetrating beyond the upper surface of the biofilm (data not shown). To evaluate electrostatic effects on diffusion, biofilms were exposed to fluorescein-conjugated dextrans bearing a net negative charge. The diffusion coefficients (see below) of these anionic probes with molecular weights of 4,000 and 70,000 were 4.97 and 0.36 $\mu m^2\ s^{-1}$, respectively, and were nearly identical to those seen for their neutral TR-dextran counterparts (see Table 2).

The mean depths of penetration ($\bar{x}^2$) of TR-dextrans, 100K-Ig, 150K-Ig, and 240K-PE into biofilms during the time intervals examined are presented in Table 1. Fifteen independent

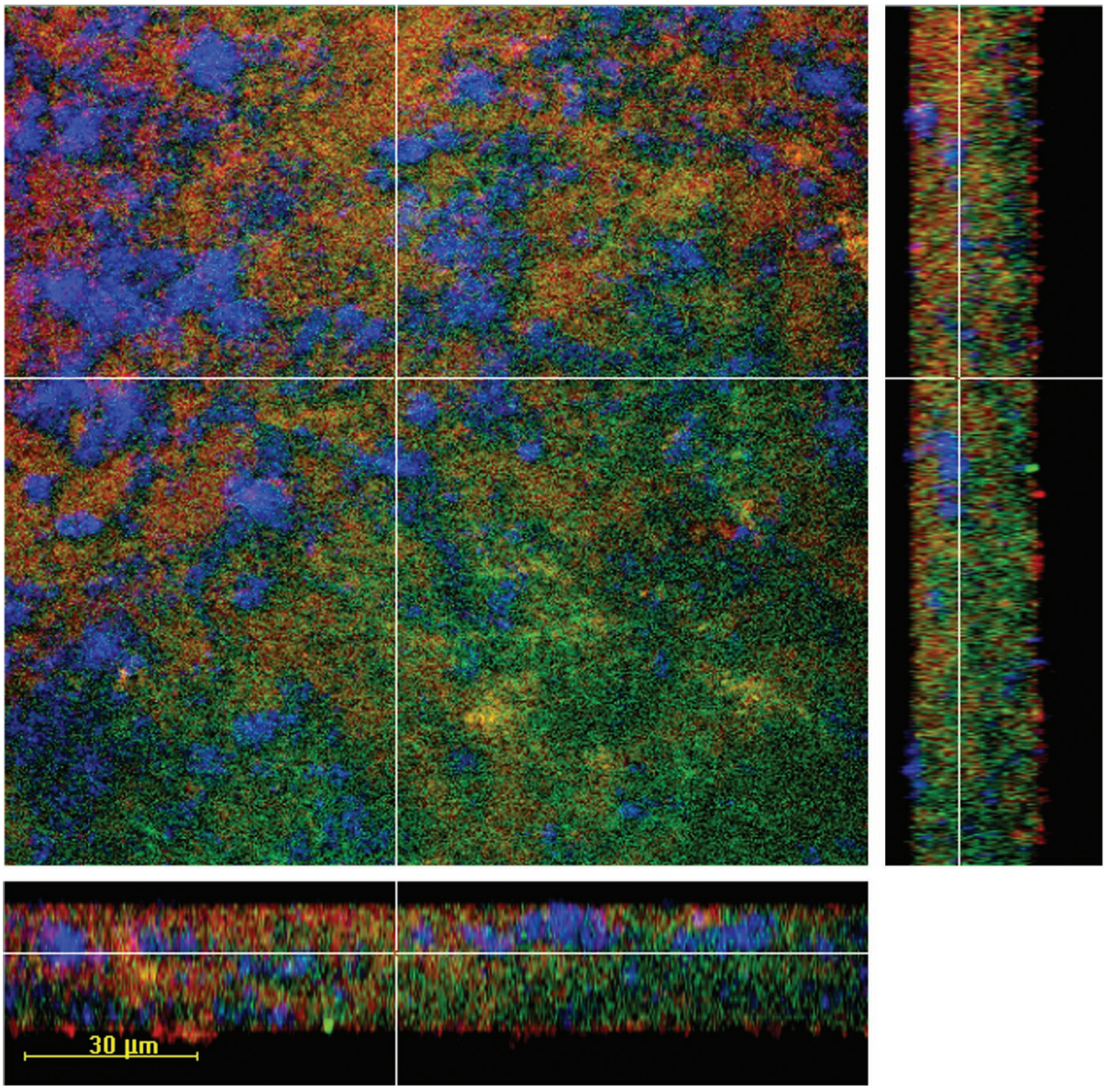

FIG. 1. CLSM images showing perpendicular *xy*, *xz*, and *yz* planes through a randomly selected point of a 64.5-h biofilm. The biofilm was stained with Syto13 for microorganisms (green), with Calcofluor for EPS (blue), and with 10K-Dex for interstitial spaces (red). Images were obtained by using a ×40 oil immersion objective.

measurements of $\bar{x}^2$ for each incubation period (Δt) for each fluorescent probe were plotted according to equation 3 (data not shown). These scattergrams yielded indices of determination (r^2) for $\bar{x}^2$ versus Δt of 0.90, 0.84, 0.90, 0.93, 0.88, 0.68, and 0.83 for the 3K-Dex, 10K-Dex, 40K-Dex, 70K-Dex, 100K-Ig, 150K-Ig, and 240K-PE probes, respectively, indicating that diffusion rates for each probe were more or less constant and did not vary substantially with biofilm depth. The data in Table 1 were used to calculate D_{bf} values (Table 2). On theoretical grounds (19), it may be shown that diffusivity is linearly proportional to the cube root of the molecular weight. Therefore, when D_{bf} was plotted against the cube root of the molecular weight, a linear relationship ($r^2 = 0.94$) was obtained over the molecular weight range of 10,000 through 240,000, but a dramatic increase in diffusivity occurred as the probe molecular weight decreased from 10,000 to 3,000 (Fig. 4).

In additional control experiments, biofilms preincubated with unlabeled dextran (molecular weight, 1,000) and then reincubated with TR-dextrans showed diffusion coefficients for the fluorescent probes nearly identical to those obtained for biofilms not treated with unlabeled dextran. Differences in measured diffusion coefficients for 3K-Dex, 10K-Dex, 40K-Dex, and 70K-Dex with and without unlabeled dextran pretreatment were -0.42, -0.01, -0.02, and -0.04 $\mu m^2\ s^{-1}$, respectively. Furthermore, extensive washing (60 min) of biofilms following incubation with TR-dextrans resulted in nearly complete removal of the dye.

The D_{bf} values were strikingly lower than the diffusion co-

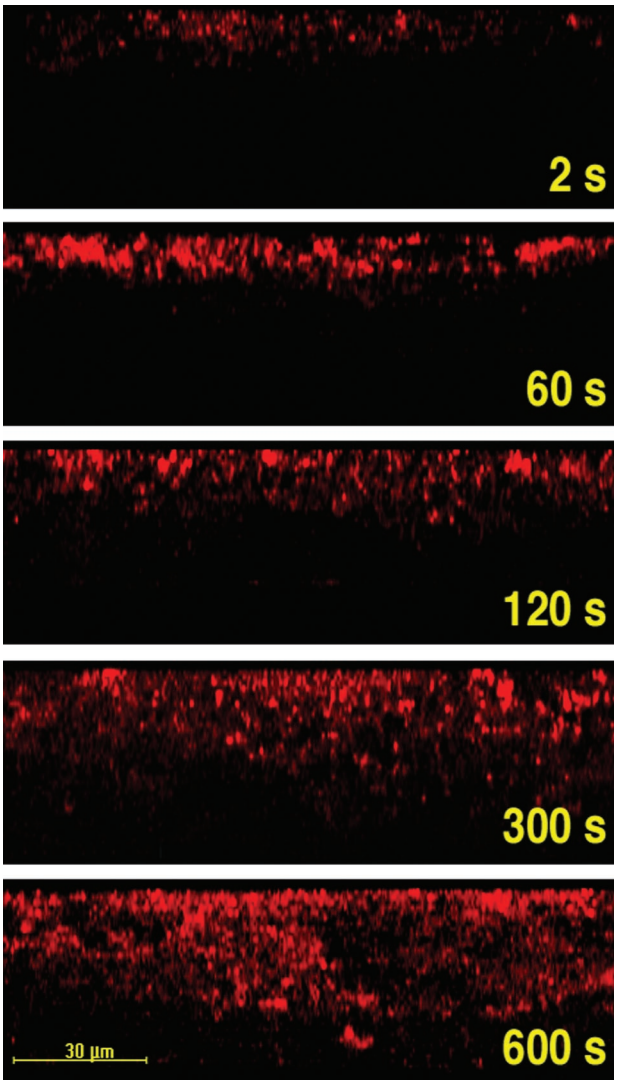

FIG. 2. Images of *xz* sections of 64.5-h biofilms showing the diffusion of 10K-Dex as a function of time (up to 600 s). Images were obtained by using a ×100 oil immersion objective.

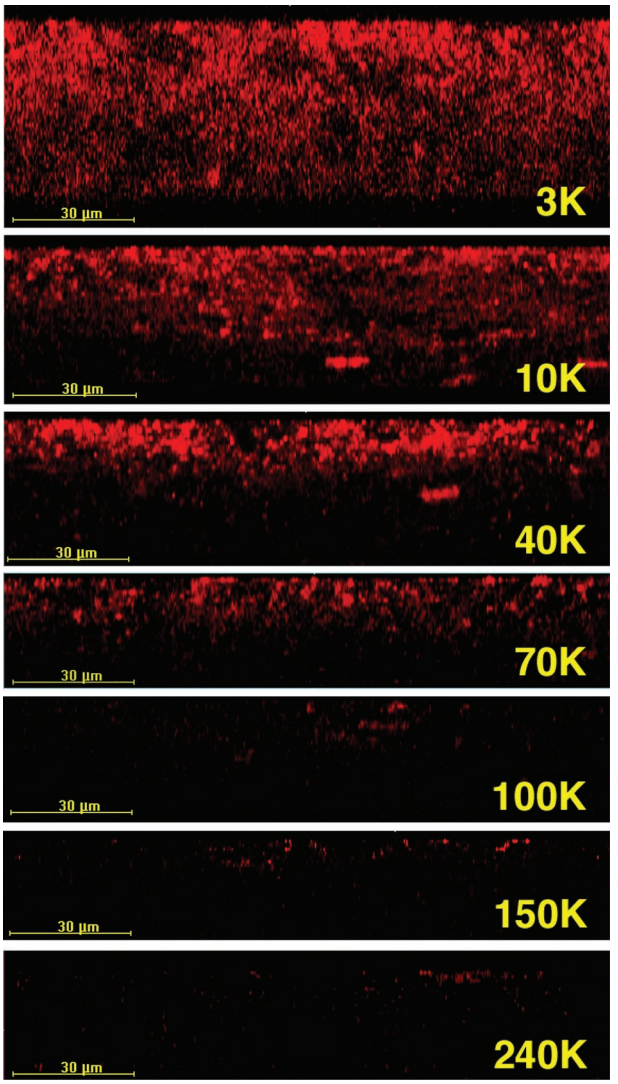

FIG. 3. *xz* sections of 64.5-h biofilms showing the diffusion of macromolecules with different molecular weights after 120 s (3K-Dex) or 600 s (probes with molecular weights of 10,000 to 240,000 [10K to 240K]).

efficients seen in bulk water or agar gels (D_w) (Table 2). Such retarded diffusion could have been due to several factors (discussed below). To assess the impact of the convoluted paths traversed by the macromolecules during biofilm penetration, tortuosity indices were calculated. The tortuosity index, defined as the square root of D_w/D_{bf}, is a measure of probe percolation through interstitial space (36). Plotting tortuosity indices for all probes (Table 2) versus probe molecular weights yielded a line for which r^2 was 0.76 (Fig. 5).

DISCUSSION

In the present study, we sought to quantify diffusion into and within a polyspecies biofilm model of supragingival plaque by investigating penetration of fluorescent probes under stagnant conditions, where convective effects on intrabiofilm transport are negligible (21). Although composed of only six microorganisms, the model was characterized by considerable morphological complexity, illustrated through the use of dyes to highlight microorganisms (Syto13), EPS (Calcofluor), and interstitial spaces (10K-Dex) (Fig. 1). Structural heterogeneity within the biofilms was expected to result in regional differences in macromolecule diffusion; therefore, diffusion measurements were always performed by using triplicate biofilms and examining five randomly selected spots per biofilm (for a total of 15 independent analyses per probe per time point). Our measurements showed that for molecular weights of up to 240,000, probe penetration depths increased linearly (or nearly so) with time (Table 1), enabling us to calculate D_{bf} values for each of the probes. The 240K-PE probe penetrated poorly into biofilms, whereas 900K-Ig collected on the surface and hardly penetrated into biofilms at all. From reported hydrodynamic radii for R-phycoerythrin (5.5 nm) (29) and IgM (14.0 nm) (40), the limiting width of these biofilm lumens can be estimated to be slightly greater than 11 nm. The finding that IgM

TABLE 1. Mean distances of penetration of fluorescent probes into artificial supragingival plaque as a function of time

Time (s)	Mean ± SD distance of penetration (μm) of the following fluorescent probe[a]:						
	3K-Dex	10K-Dex	40K-Dex	70K-Dex	100K-Lg	150K-lg	240K-PE
2	12.1 ± 2.3	11.5 ± 3.0	7.8 ± 1.6	6.2 ± 1.2	2.8 ± 0.8	3.0 ± 1.2	1.8 ± 1.5
60	28.3 ± 2.5	16.6 ± 2.1	10.7 ± 1.9	8.4 ± 1.2	5.3 ± 1.8	5.1 ± 1.5	2.7 ± 1.1
120	45.1 ± 4.0	20.2 ± 2.6	15.1 ± 2.9	10.2 ± 1.4	7.4 ± 2.2	7.1 ± 2.3	5.2 ± 1.1
300	NT	25.9 ± 3.1	19.5 ± 3.6	14.0 ± 1.8	12.1 ± 2.1	11.2 ± 3.0	7.8 ± 1.6
600	NT	30.8 ± 2.1	27.7 ± 1.6	22.8 ± 1.3	17.2 ± 2.3	13.8 ± 2.6	11.7 ± 1.7

[a] Data are based on 15 measurements. NT, not tested.

was unable to penetrate biofilms contrasts with previously reported data (17). However, in this earlier study, a growth medium with a 50:50 (vol/vol) ratio of saliva to mFUM was used, whereas in the present study, the ratio was shifted to 70:30 (vol/vol). This change in the saliva/mFUM ratio led to a more rigid biofilm with apparently different diffusion properties. Thus, altered growth conditions can profoundly affect biofilm diffusivity.

The linear relationships seen in plots of $\bar{x}^2$ versus Δt attest to the high measurement quality of each data set and indicate that there was no change in the resistance to diffusion to the extent that the probes migrated through the biofilms. Curiously, a difference of 1 order of magnitude was observed between 3K-Dex and 10K-Dex for D_{bf} (Fig. 4), whereas on theoretical grounds, a D_{bf} value of only about 1.7 was expected (Table 2). This discrepancy suggested a possible sieving effect in the biofilm brought about by a preponderance of EPS "pore" diameters wider than 2.6 nm (estimated diameter of 3K-Dex) (37) but narrower than 4.6 nm (estimated diameter of 10K-Dex) (37).

In the absence of mitigating circumstances, the diffusion coefficient of molecules in a bulk solution should decrease with the cube root of the molecular weight (19). Except for 3K-Dex, this relationship was observed for our biofilms, although the D_{bf} values indicated that diffusion rates in biofilms were much lower than those in bulk water; this attenuation effect was more pronounced at higher probe molecular weights (Table 2). Retarded diffusion has been reported for a variety of biological systems (Table 3) as well as for artificial test systems, such as hydroxypropylcellulose (7) or gel matrices consisting of cross-linked polymers (28). Lawrence et al. (26), assessing dextran diffusion in mixed-culture soil biofilms, reported D_{bf} values for 40K-Dex and 70K-Dex probes comparable to those obtained in our model of supragingival plaque. Likewise, Guiot and coworkers (18), using FCS under two-photon excitation, reported that apparent diffusion coefficients for macromolecules in monospecies biofilms were up to 50 times smaller than those in bulk water.

TABLE 2. Diffusion coefficients at 25°C of fluorescent probes in water and biofilms and calculated tortuosity indices

Probe	D_w[a] ($\mu m^2\ s^{-1}$)	D_{bf} ($\mu m^2\ s^{-1}$)	D_w/D_{bf}	Tortuosity index
3K-Dex	186	6.59	28	5.3
10K-Dex	108	0.69	157	12.5
40K-Dex	34	0.59	58	7.6
70K-Dex	30	0.36	83	9.1
100K-Lg	56	0.24	233	15.3
150K-lg	38	0.17	224	15.0
240K-PE	45	0.10	450	21.2

[a] Data were from the following sources: TR-dextrans (35), 100K-Ig (9), 150K-Ig (40), and 240K-PE (29). These data, obtained at a given temperature, were converted to D_w values at 25°C by using the relationship $D_{w,25} = (D_{w,x} \times T_{25} \times \eta_x)/(T_x \times \eta_{25})$, where T is the absolute temperature (kelvin scale) and η is the viscosity of water (14).

To what extent discrepancies between D_{bf} values determined for different biofilm models (Table 3) can be explained by methodological or analytical differences remains to be explored. Retarded diffusion could be related to increased viscosity within the biofilm mass, to selective binding of probe molecules to bacteria and/or the EPS matrix, to a highly tortuous biofilm microstructure, to entropic trapping (28), or to any combination of these factors. The viscosity of the biofilm growth medium at 25°C was determined to be 1.062 ± 0.004 (mean and standard deviation) cP, similar to that of water at the same temperature (0.890 cP). The physicochemical properties of the interstitial fluid in our biofilm model are not known but likely closely resemble those of the medium in which the biofilm is grown (18). Thus, viscosity, which appears in the denominator of the Stokes-Einstein equation (equation 4), can hardly account for the observed retardation of diffusion.

Selective binding of dextran (glucans) to biofilms containing oral streptococci, in particular, *S. sobrinus*, is well known (33), and such binding conceivably could lead to an apparent retardation of the diffusion of dextrans. Interestingly, Birmingham et al. (4), who used fluorescence photobleaching recovery methods (Table 3) to measure diffusion, detected an apparent increase in the rate of diffusion of dextrans in *S. sobrinus*-containing biofilms grown in the presence of sucrose. They explained the observed increase in the diffusion rate in terms of selective temporary binding of dextrans to enzymatic and/or nonenzymatic glucan-binding proteins, leading to significant fluorescence quenching and an apparent but physically nonexistent increase in the diffusion rate. Preincubation with unlabeled dextran failed to impede the transit of TR-dextrans through our biofilms, and the fact that the dextran, immunoglobulin, and phycoerythrin probes used all yielded reasonably linear relationships between D_{bf} and probe molecular weight indicated that selective binding of probes to EPS or microorganisms is not a significant factor in the retardation of diffusion. This conclusion is confirmed by the fact that extensive washing of the stained biofilms resulted in nearly complete removal of the dye. In addition, the two streptococcal species present in our biofilm model produce large quantities of α(1-6)- and α(1-3)-linked glucans from sucrose (23). It is very likely

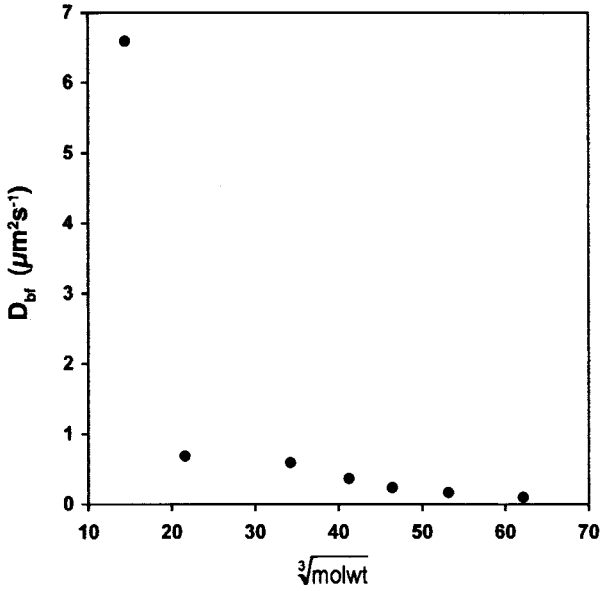

FIG. 4. Plot of D_{bf} versus the cube root of the molecular weight of fluorescent probes over the molecular weight range of 3,000 to 240,000. A linear relationship ($r^2 = 0.94$) between D_{bf} and the cube root of the molecular weight was seen for the molecular weight range of 10,000 to 240,000.

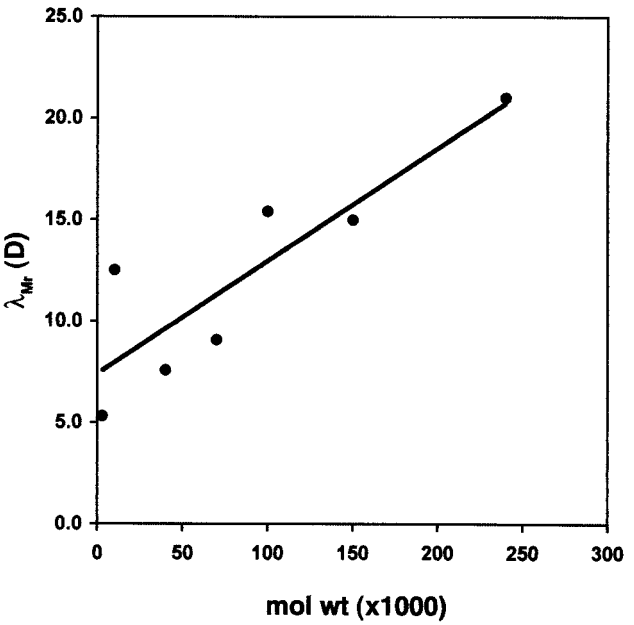

FIG. 5. Plot of tortuosity index [λ_{Mr} (D)] versus probe molecular weight (3,000 to 240,000). The approximately linear correspondence between the tortuosity index and molecular weight is evidence for the role of tortuosity in the retardation of probe diffusion through biofilms.

that these glucans continuously bind to and saturate whatever streptococcal glucan-binding sites may exist in the biofilm.

Tortuosity seems the most likely explanation for the observed discrepancy between the diffusion of probes in biofilms and that in bulk water: a molecule traversing a highly convoluted three-dimensional route laid out by interstitial voids in a matrix will be delayed in comparison to a molecule showing free diffusion in bulk water. The extracellular space of the biofilm comprises an EPS-rich hydrogel of variable porosity; the larger the probe, the more often it will encounter a pore too narrow to allow it to pass. In such cases, diffusion into the biofilm (along the *z* axis) can proceed only if the probe backtracks until it encounters a pore sufficiently wide to permit penetration deeper into the biofilm.

The relationship between the incidence of dental caries and the properties of supragingival plaque is complex. The formation of gelatinous biofilms on teeth is a necessary condition for the formation of carious lesions in vivo. The same is true for lesions formed in vitro with exogenous acids (24). Such observations led to the empirical conclusion that selective retardation of diffusion is a prerequisite for carious demineralization of enamel (13). The diffusion properties of dental plaque are governed mainly by two interactive factors: microbial composition and diet (composition and frequency of consumption). It has been postulated that the nature and amounts of extracellular glucans produced by oral streptococci from sucrose in dental plaque are major pathogenic determinants retarding acid diffusion (22). Subjects intolerant of high fructose levels cover their carbohydrate intake through starch and avoid

TABLE 3. Diffusion coefficients determined with various biological systems

Probe (mol wt, 10^3)	Diffusion coefficient, $\mu m^2\ s^{-1}$, determined with the following biological system (reference):						
	Our system	Mixed-species oral biofilm in vitro (4)	Mixed-species biofilm in vitro (11)	Single-species biofilm in vitro (6)	Mixed-species soil biofilm in vitro (26)	Rat cerebral cortex slices (37)	Xenopus neuron cell cultures (39)
Dextran (3)	6.59					81	
Dextran (4)					3.1		
Dextran (10)	0.69	43.8		196		51	
Lactalbumin (15)							97.8
Dextran (40)	0.59	49.4			1.7	9.1	
Ovalbumin (45)							79.1
Bovine serum albumin (60)							67.7
Dextran (70)	0.36			144	1.1	7.5	
IgG (150)	0.17		65				
Phycoerythrin (240)	0.1		3.9				

sweet-tasting mono- and disaccharides; compared to subjects without this intolerance, their caries incidence is low (31). Epidemiological findings point in the same direction. Before the massive increase in sucrose consumption that started in Europe in about 1850, starch was the main dietary carbohydrate and the incidence of dental caries was modest (34). The low cariogenic potential of starch was explained by its slow diffusion into plaque, after which the starch polymers must be cleaved by salivary amylase to maltotriose, maltose, or glucose to become accessible to fermenting bacteria and to manifest their full acidogenic potential (27, 44). Questions related to the effect of diffusion in dental plaque may now be addressed experimentally with biofilm models or models of dental plaque formed in situ. If measurements of enamel demineralization are used as additional experimental parameters, further relevant insights into the pathogenic mechanisms of dental caries can be expected.

ACKNOWLEDGMENTS

We thank T. Bächi and M. Höchli at the Central Electron Microscopy Laboratory of the University of Zürich for use of the confocal laser scanning microscope, G. Stark of the University of Konstanz (Konstanz, Germany) for useful discussions on diffusion and critical review of the manuscript, and A. Meier and V. Osterwalder for excellent technical assistance.

REFERENCES

1. **Beuling, E. E., D. van Dusschoten, P. Lens, J. C. van den Heuvel, H. Van As, and S. P. P. Ottengraf.** 1998. Characterization of the diffusive properties of biofilms using pulsed field gradient-nuclear magnetic resonance. Biotechnol. Bioeng. **60:**283–291.
2. **Beyenal, H., Z. Lewandowski, C. Yakymyshyn, B. Lemeley, and J. Wehri.** 2000. Fiber-optic microsensors to measure backscattered light intensity in biofilms. Appl. Optics **39:**3408–3412.
3. **Beyenal, H., A. Tanyolaç, and Z. Lewandowski.** 1998. Measurement of local effective diffusivity in heterogeneous biofilms. Water Sci. Technol. **38:**171–178.
4. **Birmingham, J. J., N. P. Hughes, and R. Treloar.** 1995. Diffusion and binding measurements within oral biofilms using fluorescence photobleaching recovery methods. Philos. Trans. R. Soc. Lond. Ser. B **350:**325–343.
5. **Bryers, J. D., and F. Drummond.** 1996. Local mass transfer coefficients in bacterial biofilms using fluorescence recovery after photobleaching (FRAP), p. 196–204. *In* R. H. Wijffels, R. M. Buitelaar, C. Bucke, and J. Tramper (ed.), Immobilized cells: basics and applications. Elsevier, Amsterdam, The Netherlands.
6. **Bryers, J. D., and F. Drummond.** 1998. Local macromolecule diffusion coefficients in structurally non-uniform bacterial biofilms using fluorescence recovery after photobleaching (FRAP). Biotechnol. Bioeng. **60:**462–473.
7. **Bu, Z., and P. S. Russo.** 1994. Diffusion of dextran in aqueous (hydroxypropyl)cellulose. Macromolecules **27:**1187–1194.
8. **Carlsson, J.** 1997. Bacterial metabolism in dental biofilms. Adv. Dent. Res. **11:**75–80.
9. **Carrasco, B., J. Garcia de la Torre, K. G. Davis, S. Jones, D. Athwal, C. Walters, D. R. Burton, and S. E. Harding.** 2001. Crystallohydrodynamics for solving the hydration problem for multi-domain proteins: open physiological conformations for human IgG. Biophys. Chem. **93:**181–196.
10. **Costerton, J. W., Z. Lewandowski, D. E. Caldwell, D. R. Korber, and H. M. Lappin-Scott.** 1995. Microbial biofilms. Annu. Rev. Microbiol. **49:**711–745.
11. **de Beer, D., P. Stoodley, and Z. Lewandowski.** 1997. Measurement of local diffusion coefficients in biofilms by microinjection and confocal microscopy. Biotechnol. Bioeng. **53:**151–158.
12. **Dibdin, G. H.** 1981. Diffusion of sugars and carboxylic acids through human dental plaque in vitro. Arch. Oral Biol. **26:**515–523.
13. **Dibdin, G. H.** 1984. A brief survey of recent in vitro work on diffusion of small ions and molecules in dental plaque, p. 191–198. *In* B. Guggenheim (ed.), Cariology today. Karger, Basel, Switzerland.
14. **Einstein, A.** 1905. Über die von der molekular-kinetischen Theorie der Wärme geforderte Bewegung von in ruhenden Flüssigkeiten suspendierten Teilchen. Ann. Phys. **17:**549–560.
15. **Gmür, R., and B. Guggenheim.** 1983. Antigenic heterogeneity of *Bacteroides intermedius* as recognized by monoclonal antibodies. Infect. Immun. **42:**459–470.
16. **Guggenheim, B., E. Giertsen, P. Schüpbach, and S. Shapiro.** 2001. Validation of an in vitro biofilm model of supragingival plaque. J. Dent. Res. **80:**363–370.
17. **Guggenheim, M., S. Shapiro, R. Gmür, and B. Guggenheim.** 2001. Spatial arrangements and associative behavior of species in an in vitro oral biofilm model. Appl. Environ. Microbiol. **67:**1343–1350.
18. **Guiot, E., P. Georges, A. Brun, M. P. Fontaine-Aupart, M. N. Bellon-Fontaine, and R. Briandet.** 2002. Heterogeneity of diffusion inside microbial biofilms determined by fluorescence correlation spectroscopy under two-photon excitation. Photochem. Photobiol. **75:**570–578.
19. **Haglund, B. O., D. E. Wurster, L.-O. Sundelöf, and S. M. Upadrashta.** 1996. Effect of SDS micelles on rhodamine-B diffusion in hydrogels. J. Chem. Educ. **73:**889–893.
20. **Hermanowicz, S. W.** 2003. Biofilm structure: an interplay of models and experiments, p. 32–47. *In* S. Wuertz, P. L. Bishop, and P. A. Wilderer (ed.), Biofilms in wastewater treatment—an interdisciplinary approach, in press. International Water Association Publishing, London, United Kingdom.
21. **Hermanowicz, S. W., U. Schindler, and P. Wilderer.** 1995. Fractal structure of biofilms: new tools for investigation of morphology. Water Sci. Technol. **32:**99–105.
22. **Hojo, S., M. Huguchi, and S. Araya.** 1976. Glucan inhibition of diffusion in plaque. J. Dent. Res. **55:**169.
23. **Hotz, P., B. Guggenheim, and R. Schmid.** 1972. Carbohydrates in pooled dental plaque. Caries Res. **6:**103–121.
24. **Ingram, G. S., and L. M. Silverstone.** 1981. A chemical and histological study of artificial caries in human dental enamel in vitro. Caries Res. **15:**393–398.
25. **Kuehn, M., M. Mehl, M. Hausner, H. J. Bungartz, and S. Wuertz.** 2001. Time-resolved study of biofilm architecture and transport processes using experimental and simulation techniques: the role of EPS. Water Sci. Technol. **43:**143–150.
26. **Lawrence, J. R., G. M. Wolfaardt, and D. R. Korber.** 1994. Determination of diffusion coefficients in biofilms by confocal laser microscopy. Appl. Environ. Microbiol. **60:**1166–1173.
27. **Lingström, P., J. van Houte, and S. Kashket.** 2000. Food starches and dental caries. Crit. Rev. Oral Biol. Med. **11:**366–380.
28. **Liu, L., P. Li, and S. A. Asher.** 1999. Entropic trapping of macromolecules by mesoscopic periodic voids in a polymer hydrogel. Nature **397:**141–144.
29. **MacColl, R., L. E. Eisele, E. C. Williams, and S. S. Bowser.** 1996. The discovery of a novel R-phycoerythrin from an Antarctic red alga. J. Biol. Chem. **271:**17157–17160.
30. **Marsh, P. D., and D. J. Bradshaw.** 1997. Physiological approaches to the control of oral biofilms. Adv. Dent. Res. **11:**176–185.
31. **Marthaler, T. M., and E. R. Froesch.** 1967. Hereditary fructose intolerance. Dental status of eight patients. Br. Dent. J. **123:**597–599.
32. **McNee, S. G., D. A. M. Geddes, D. A. Weetman, D. Sweeney, and J. A. Beeley.** 1982. Effect of extracellular polysaccharides on diffusion of NaF and [^{14}C]-sucrose in human dental plaque and in sediments of the bacterium *Streptococcus sanguis* 804 (NCTC 10904). Arch. Oral Biol. **27:**981–986.
33. **Mooser, G., and C. Wong.** 1988. Isolation of a glucan-binding domain of glucosyltransferase (1,6-α-glucan synthase) from *Streptococcus sobrinus*. Infect. Immun. **56:**880–884.
34. **Newbrun, E.** 1982. Sugar and dental caries: a review of human studies. Science **217:**418–423.
35. **Nicholson, C.** 2001. Diffusion and related transport mechanisms in brain tissue. Rep. Prog. Phys. **64:**815–884.
36. **Nicholson, C., and J. M. Phillips.** 1981. Ion diffusion modified by tortuosity and volume fraction in the extracellular microenvironment of the rat cerebellum. J. Physiol. **321:**225–257.
37. **Nicholson, C., and L. Tao.** 1993. Hindered diffusion of high molecular weight compounds in brain extracellular microenvironment measured with integrative optical imaging. Biophys. J. **65:**2277–2290.
38. **Picioreanu, C.** 1999. Multidimensional modeling of biofilm structure. Ph.D. thesis. Delft University of Technology, Delft, The Netherlands.
39. **Popov, S., and M. Poo.** 1992. Diffusional transport of macromolecules in developing nerve processes. J. Neurosci. **12:**77–85.
40. **Radomsky, M. L., K. J. Whaley, R. A. Cone, and W. M. Saltzman.** 1990. Macromolecules released from polymers: diffusion into unstirred fluids. Biomaterials **11:**619–624.
41. **Ramsing, N. B., M. Kühl, and B. B. Jørgensen.** 1993. Distribution of sulfate-reducing bacteria, O_2, and H_2S in photosynthetic biofilms determined by oligonucleotide probes and microelectrodes. Appl. Environ. Microbiol. **59:**3840–3849.
42. **Rasmussen, K., and Z. Lewandowski.** 1998. Microelectrode measurements of local mass transport rates in heterogeneous biofilms. Biotechnol. Bioeng. **59:**302–309.
43. **Santegoeds, C. M., L. R. Damgaard, C. Hesselink, J. Zopfi, P. Lens, G. Muyzer, and D. De Beer.** 1999. Distribution of sulfate-reducing and methanogenic bacteria in anaerobic aggregates determined by microsensor and molecular analyses. Appl. Environ. Microbiol. **65:**4618–4629.
44. **Scannapieco, F. A., G. Torres, and M. J. Levine.** 1993. Salivary α-amylase: role in dental plaque and caries formation. Crit. Rev. Oral Biol. Med. **4:**301–307.
45. **Shapiro, S., E. Giertsen, and B. Guggenheim.** 2002. An in vitro oral biofilm model for comparing efficacies of antimicrobial mouthrinses. Caries Res. **36:**93–100.

46. **Stoodley, P., J. D. Boyle, and H. M. Lappin-Scott.** 1999. Biofilm structure and behaviour: influence of hydrodynamics and nutrients, p. 63–72. *In* H. H. Newman and M. Wilson (ed.), Dental plaque revisited: oral biofilms in health and disease. Bioline, Cardiff, United Kingdom.
47. **Suci, P. A., G. G. Geesey, and B. J. Tyler.** 2001. Integration of Raman microscopy, differential interference contrast microscopy, and attenuated total reflection Fourier transform infrared spectroscopy to investigate chlorhexidine spatial and temporal distribution in *Candida albicans* biofilms. J. Microbiol. Methods **46:**193–208.
48. **Tatevossian, A.** 1979. Diffusion of radiotracers in human dental plaque. Caries Res. **13:**154–162.
49. **Taylor, J. R.** 1997. An introduction to error analysis. The study of uncertainties in physical measurements, 2nd ed. University Science Books, Sausalito, Calif.
50. **Thurnheer, T., B. Guggenheim, and R. Gmür.** 1997. Characterization of monoclonal antibodies for rapid identification of *Actinomyces naeslundii* in clinical samples. FEMS Microbiol. Lett. **150:**255–262.
51. **von Smoluchowski, M.** 1906. Zur kinetischen Theorie der Brownschen Molekularbegegung und der Suspension. Ann. Phys. **21:**756–780.
52. **Vogt, M., H. C. Flemming, and W. S. Veeman.** 2000. Diffusion in *Pseudomonas aeruginosa* biofilms: a pulsed field gradient NMR study. J. Biotechnol. **77:**137–146.